

## LARGE-SCALE CURRENTS AND SEA-BOTTOM ELEVATION CHANGE DEVELOPED BY WINTER STORMS

Shinji Sato

### 1. INTRODUCTION

Severe storms are frequently generated in winter along coasts on the Japan Sea side, which are developed by strong northwestern wind caused by periodic passages of low-pressure systems across the sea. The winter storm generally persists for several days, generating strong winds and large waves from northwest. During the storm, strong alongshore currents are also observed in the offshore region, which may continue to flow over a couple of days. The estimation of the currents, which are almost as strong as nearshore currents in surf zone, is important since those currents will exert strong influence on various coastal processes, such as the propagation of wind waves and the sand transport during the storm.

In order to evaluate long-term large-scale coastal evolution, it is essential to understand sand transport mechanisms outside of the surf zone. Although sediment transport outside of surf zone is relatively weak compared with that in surf zone, various strong currents were observed near the bottom which may contribute to long-term sediment transport ( Niedroda and Swift, 1991 ). These currents are generated by the global wind system, the gravity anomaly due to the relative motion of the sun and the moon, and the difference in the sea water density. Sato (1995) showed that the strong alongshore currents observed near the bottom of Niigata coast at the depth of 15m were identified as large-scale coastal boundary currents which were developed and maintained by the wind stress and the Coriolis force.

The objective of this study is to investigate the dynamics of waves, currents and sand movement during winter storms. The mechanism of the generation of the strong large-scale currents in the offshore region is described on the basis of field data as well as numerical experiments. The effects of the offshore currents on the nearshore currents and the sediment movement will be described in detail.

### 2. ANALYSIS OF FIELD DATA

Field investigations were performed at Ishikawa and Niigata coasts facing the Japan Sea ( see Fig. 1 ) during the period from December 1994 to February 1995. On both coasts, the beaches are covered with fine sand and the bottom topographies are of simple contour lines with mean bed slope about 1/100. Three pairs of ultrasonic wave gages and current meters were installed on each coast.

On Ishikawa coast, two sets of wave gages and current meters were situated at the depths of 10.6m and 15.1m off Tokumitsu. Another set was installed at the depth of 15.1m off Shimbori river-mouth, which was 30km to the southwest of Tokumitsu, in order to confirm the alongshore scale of the currents in the offshore region. The elevation of the current meters was 0.6m above the bottom. In addition to the measurements of waves and currents, the bed elevation was monitored by an optical bed elevation sensor at Tokumitsu 15.1m. The movement of sand at Tokumitsu 15.1m was also investigated by fluorescent sand tracer test. The fluorescent sand was placed on December 23, 1994 and sampled on January 17, 1995 at eight points

---

\* Dr. Eng., Senior Researcher, Coastal Eng. Division, Public Works Research Institute,  
1 Asahi, Tsukuba, Ibaraki 305, JAPAN (sato@pwri.go.jp)

situated in a circular area with 2m radius around the injection point. Small amount of fluorescent sand was identified in all the samples except for one obtained at the south of the injection point, indicating significant sand movement at the site.

Temporal variations of data obtained at Tokumitsu 15.1m were shown in Fig. 2. The upper part of Fig. 2 shows mean water level  $\bar{\eta}$ , atmospheric pressure  $\eta_p$ , the significant wave height  $H_{1/3}$ , the significant wave period  $T_{1/3}$ , current velocity  $u$  near the bottom, wind velocity  $W$ . The atmospheric pressure  $p_0$  was converted to the equivalent water level change  $\eta_p$  by  $\eta_p = (\bar{p}_0 - p_0)/(\rho_w g)$ , where  $\rho_w$  is the density of sea water,  $g$  the gravity acceleration and  $\bar{p}_0$  the mean atmospheric pressure. A few storms were generated in the observation period by the passage of low-pressure system across the Japan Sea. The rise in the mean water level as well as the generation of strong waves and currents were observed during storms. The currents, which exceeded 40cm/s on January 5 and 10, were mostly developed in the alongshore direction. Northeast ward currents were especially strong since strong winds from W to NW blew obliquely to the shoreline.

The lower part of Fig. 2 shows variations of the bed elevation  $z_b$ , the skewness  $\sqrt{\beta_{1u}}$  in near-bottom velocity  $u_b$  and the Shields parameter  $\Psi$  defined as follows:

$$\sqrt{\beta_{1u}} = \frac{(u_b - \bar{u}_b)^3}{[(u_b - \bar{u}_b)^2]^{3/2}} \quad (1)$$

$$\Psi = \frac{1}{2} f_w \frac{\hat{u}_b^2}{(\rho_s/\rho_w - 1)gD} \quad (2)$$

where  $f_w$  is the wave friction factor,  $\hat{u}_b$  the velocity amplitude near the bottom estimated in terms of the significant wave height,  $\rho_s$  the density of sand particles and  $D$  the diameter of sand particles. The diameter of sand particles was estimated at 0.15mm from sieve analysis of sand samples. The change in bed elevation was significant when the Shields parameter exceeded 0.1. The bed elevation showed a sudden decrease at the early stage of storm when the velocity skewness and the Shields parameter increased rapidly. After the sudden scour of bed, the bed was recovered gradually in a couple of days. The sudden scour of the bed was considered to be due to the spatial imbalance in the shoreward transport of sediment which was enhanced by the asymmetric wave orbital motion under steep waves observed at the early stage of the storm. It is also noticed that significant change in bed elevation does not always occur under high waves, when the Shields parameter is on the order of unity.

Sato (1995) showed on the basis of field data obtained at Niigata coast that strong northwestern wind during a winter storm caused a rise in sea water level near the shoreline as well as the generation of strong alongshore currents. Figure 3 shows the relationship between the alongshore component of the current velocity and that of the wind velocity for the data obtained at Tokumitsu. In order to identify the effect of obliquely incident waves on the currents, the plot was classified in terms of  $H_s$  defined as follows:

$$H_s = H_{1/3} \frac{\vec{k} \cdot \vec{s}}{|\vec{k}|} \quad (3)$$

where  $\vec{k}$  is the wavenumber vector and  $\vec{s}$  the unit vector parallel to the shoreline. Longshore currents with  $u_s > 0$  will be developed in surf zone when  $H_s > 0$ . It is noticed in Fig. 3 that the magnitude of the current velocity increases as wind velocity increases. However, the current velocities at the depth of 10.6m are sensitive to the wave height. This is because the currents at the depth of 10.6m were affected by longshore currents developed in surf zone. It is also noted that the current velocities at the depth of 15.1m tends to increase as wave height increases, although it is less obvious than those at 10.6m.

### 3. LARGE-SCALE CURRENTS DEVELOPED BY WINDS AND WAVES

#### (1) Numerical Model

Numerical experiments were performed in order to determine the essential physical mechanisms involved in the generation of the strong alongshore currents. The currents and the mean water level change induced by strong winds were numerically simulated on the basis of the following depth-integrated mass and momentum equations:

$$\frac{\partial \eta}{\partial t} + \frac{\partial Q_x}{\partial x} + \frac{\partial Q_y}{\partial y} = 0 \quad (4)$$

$$\frac{\partial Q_x}{\partial t} + \frac{\partial}{\partial x} \left( \frac{Q_x^2}{d} \right) + \frac{\partial}{\partial y} \left( \frac{Q_x Q_y}{d} \right) - f Q_y + g d \frac{\partial \eta}{\partial x} + \frac{d}{\rho_w} \frac{\partial p_0}{\partial x} + \frac{1}{\rho_w} \left( \frac{\partial S_{xx}}{\partial x} + \frac{\partial S_{xy}}{\partial y} \right) - \frac{\tau_{sx}}{\rho_w} + \frac{\tau_{bx}}{\rho_w} - \epsilon \left( \frac{\partial^2 Q_x}{\partial x^2} + \frac{\partial^2 Q_x}{\partial y^2} \right) = 0 \quad (5)$$

$$\frac{\partial Q_y}{\partial t} + \frac{\partial}{\partial x} \left( \frac{Q_x Q_y}{d} \right) + \frac{\partial}{\partial y} \left( \frac{Q_y^2}{d} \right) + f Q_x + g d \frac{\partial \eta}{\partial y} + \frac{d}{\rho_w} \frac{\partial p_0}{\partial y} + \frac{1}{\rho_w} \left( \frac{\partial S_{yx}}{\partial x} + \frac{\partial S_{yy}}{\partial y} \right) - \frac{\tau_{sy}}{\rho_w} + \frac{\tau_{by}}{\rho_w} - \epsilon \left( \frac{\partial^2 Q_y}{\partial x^2} + \frac{\partial^2 Q_y}{\partial y^2} \right) = 0 \quad (6)$$

where  $Q_x$  and  $Q_y$  are flow rates in the  $x$  and  $y$  directions respectively,  $\eta$  the surface elevation,  $d (= h + \eta)$ ,  $h$  the still water depth) the total depth,  $\tau_s$  and  $\tau_b$  the wind stress and the bottom shear stress respectively,  $S_{xx}$ ,  $S_{xy}$  and  $S_{yy}$  the radiation stresses,  $f (= 2\omega \sin \phi)$ , where  $\omega$  is the angular frequency of earth rotation and  $\phi$  the latitude) the Coriolis coefficient and  $\epsilon$  the horizontal eddy viscosity.

The computational domain was a rectangular area of 100km in the alongshore direction and 30km in the cross-shore direction. The sea bottom slope was set at 1/100 which simulated the mean beach slope of Ishikawa and Niigata coasts. The governing equations were numerically integrated by an efficient ADI algorithm (Sato, 1995). The grid size was 200m in an area within a distance of 3km from the shoreline and 1km elsewhere. The wind speed was assumed to be uniform in the entire domain. Temporal wind variations observed on the coast were used as the input to the model, which simulated the generation of large-scale currents in the offshore region as well as nearshore currents in surf zone.

The surface stress due to wind was estimated by,

$$\vec{\tau}_s = \rho_a C_a \vec{W} |\vec{W}| \quad (7)$$

where  $\rho_a$  is the density of air and  $C_a$  is the drag coefficient of sea surface. The bottom shear stress was modeled by Manning's formula,

$$\vec{\tau}_b = \frac{\rho_w g n^2}{d^{1/3}} \vec{i} |\vec{i}| \quad (8)$$

where  $n$  is a roughness parameter, which was determined at  $n = 0.026$  ( $m^{1/3}s$ ) typically used in storm surge simulation. On the basis of the data obtained at Tokumitsu in which the currents are regarded equilibrium where the surface drag due to wind balanced the bottom shear stress, the value of  $C_a$  was estimated to be  $C_a = 0.001$ . The value is consistent with the laboratory measurements of wind waves (Honda and Mitsuyasu, 1980).

The radiation stress was estimated from random wave shoaling model presented by Goda and Watanabe (1990) which showed that the cross-shore distribution of longshore currents could be simulated by considering wave randomness without using unrealistic large value for the eddy viscosity  $\epsilon$ . The offshore wave height distribution was determined as the Rayleigh distribution and the change in the wave height distribution was computed by using random wave breaking model of Goda(1975). The distribution of the radiation stress was then estimated from that of  $H_{rms}$ .

Longuet-Higgins (1970) introduced the following formula for eddy viscosity,

$$\epsilon = N l_x \sqrt{g h} \quad (9)$$

where  $N (< 0.016)$  is a non-dimensional coefficient and  $l_x$  is the distance from the shoreline. When the eddy viscosity is evaluated for a typical storm condition observed on Ishikawa and Niigata coasts, the eddy viscosity is evaluated at the order of 25  $m^2/s$  for waves with significant wave height of 4m breaking on a 1/100 sloping beach. In the present study, since the radiation stress was estimated with the effect of wave randomness, the value of eddy viscosity was set at a small value of 1  $m^2/s$  which provided stable computation.

## (2) Effect of Waves

In surf zone, longshore currents will be developed by obliquely incident waves. Wind driven currents, on the other hand, will be generated in the direction of winds, so that the currents outside of surf zone and

those in surf zone may be opposite when the wave direction and the wind direction are opposite with respect to the sea bottom contours. Figure 4 illustrates variations of waves, currents and winds observed at Niigata coast from January 30 to February 2, 1996. On January 31, all the currents at  $h = 8.8\text{m}$ ,  $15.4\text{m}$  and  $20.0\text{m}$  were directed to the northeast owing to strong winds from the west. However, after February 1 when waves from NNW increased their heights, the currents direction changed to southwest and west. The reversal of the currents originated from surf zone and gradually extended to the offshore region.

Figure 5 shows the currents calculated for the condition of Fig. 4. The currents illustrated on the top are those computed under the condition in which only winds are considered; the radiation stress terms were omitted in the momentum equation and  $\tau_s$  was estimated by using Eq. (7). The currents computed with radiation stress terms are shown in the middle of Fig. 5. When only winds were considered, northeastern currents were developed during the whole period at all the points. When radiation stresses were included, the reversal of the currents was simulated at  $h = 8.8\text{m}$ . However, the direction of the currents at  $h = 15.4\text{m}$  and  $20.0\text{m}$  was unchanged. Since the significant wave height during this period was  $4\text{m}$  at most, longshore currents would not be developed in the offshore region deeper than  $15\text{m}$ . The reversal of the currents observed after February 1 is therefore considered to be due to the effect of breaking of surface waves. Although the importance of the momentum transfer from the wave motion to the mean motion has been pointed out ( Melville and Rapp, 1985; Melsom, 1996 ), quantitative description is yet to be developed. In the present study, the effect of the surface wave breaking on the development of the currents was incorporated in a rough approach by considering an additional surface stress in the direction of wave direction. Since stronger momentum transfer will take place under larger waves, the dimensional argument leads to the following equation:

$$\vec{\tau}_s = \rho_a C_a \vec{W} |\vec{W}| + \rho_w C_w g H_{1/3} \frac{\vec{k}}{|\vec{k}|} \quad (10)$$

where  $\vec{k}$  is the wavenumber vector and  $C_w$  is a non-dimensional coefficient whose value was evaluated at  $C_w = 1.0 \times 10^{-5}$  on the basis of the comparison of simulated currents with field data. The currents simulated by using Eq. (10) were illustrated on the bottom of Fig. 5 where the reversal of the currents after February 1 were successfully simulated even in the offshore region. It is also noticed that the currents at  $h = 8.8\text{m}$  were directed slightly offshore owing to the effects of undertow.

Figure 6 illustrates the change in bottom topography observed around Kanazawa Port. Wave records indicated that the direction of the net longshore transport on this coast was from the north to the south. Before the construction of the port, the bottom contours were almost parallel to the shoreline. In 1992, since the longshore transport was blocked by the port construction, the shoreline was curved with significant accretion observed on the north side of jetties. However, in the offshore region, significant accretion was observed on the south side of the breakwater, which is considered to be due to the large-scale currents described in the present study.

#### 4. CONCLUSIONS

Field data of waves, currents, winds and bed elevation change obtained at Ishikawa and Niigata coasts facing the Japan Sea were analyzed and compared with numerical simulation. Major conclusions are as follows: (1) Strong alongshore currents as well as water level rise were developed after the passage of a low-pressure system. (2) Numerical simulation confirmed that the currents were driven by the wind stress and the Coriolis force. (3) The currents interacted with nearshore currents developed in surf zone. (4) The bed in the offshore region was observed to be scoured significantly by steep waves at the early stage of a storm.

It was also suggested that the large-scale currents could be responsible for large-scale evolution of coastal topography. Further investigation is needed to estimate the effect quantitatively.

#### 5. REFERENCÉS

- Honda, T. and H. Mitsuyasu (1980): Laboratory study on the effects of wind on sea surface, Proc. 27th Japanese Conf. on Coastal Eng., pp. 90-93 ( in Japanese ).  
 Goda, Y. (1975): Irregular wave deformation in the surf zone, Coastal Eng. in Japan, Vol. 18, pp. 13-26.

- Goda, Y. and N. Watanabe (1991): A longshore current formula for random breaking waves, Coastal Eng. in Japan, Vol. 34, No.2, pp. 159-175.
- Longuet-Higgins, M.S. (1970): Longshore currents generated by obliquely incident sea waves, J. Geophys. Res., Vol. 75, pp. 6778-6801.
- Melsom, A. (1996): Effects of wave breaking on the surface drift, J. Geophys. Res., Vol. 101, No. C5, pp. 12071-12078.
- Melville, W.K. and R.J. Rapp (1985): Momentum flux in breaking waves, Nature, Vol. 317, No. 10, pp. 514-516.
- Niedroda, A.W. and D.J.P. Swift (1991): Shoreface processes, in Handbook of Coastal and Ocean Engineering, Gulf Publishing Company, pp. 735-770.

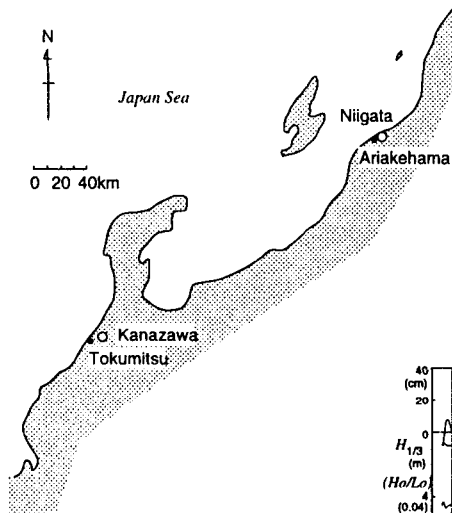


Fig. 1 Field observation sites

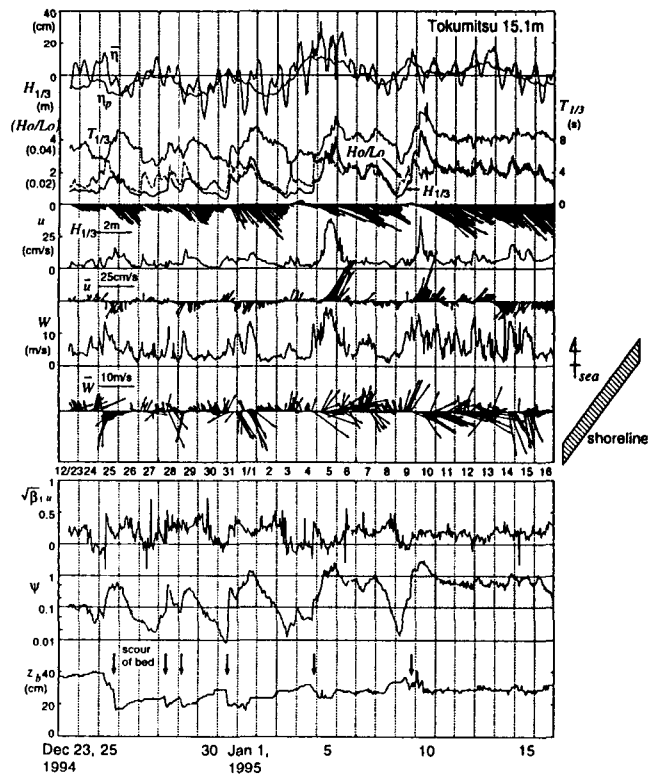


Fig. 2 Temporal variation of winds, waves, currents and bottom elevation at Ishikawa coast

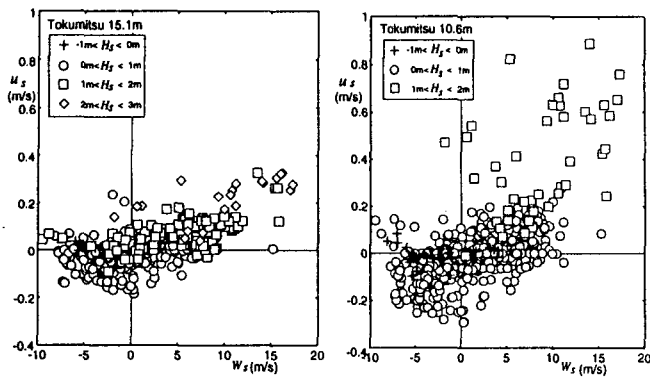


Fig. 3 Relationship between alongshore components of current velocity and wind velocity

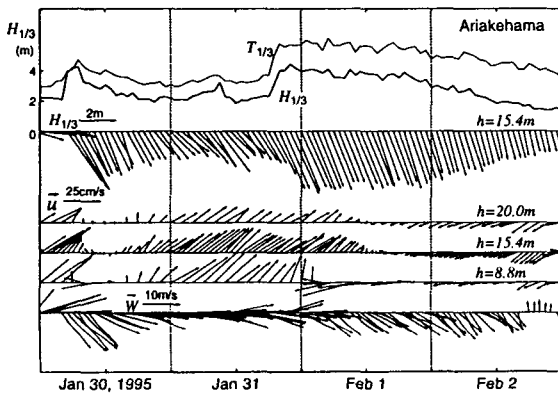


Fig. 4 Distribution of currents at Niigata coast

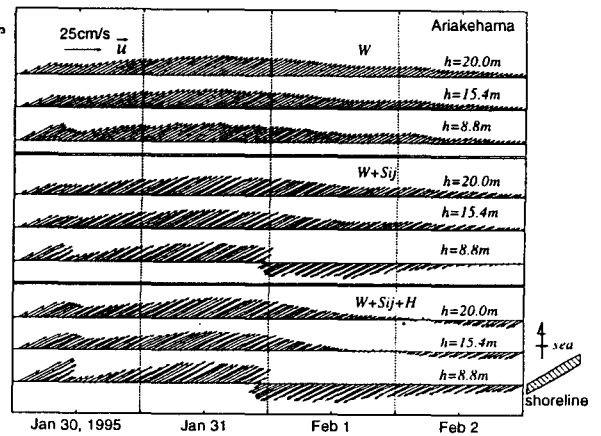


Fig. 5 Distribution of currents computed for Niigata coast

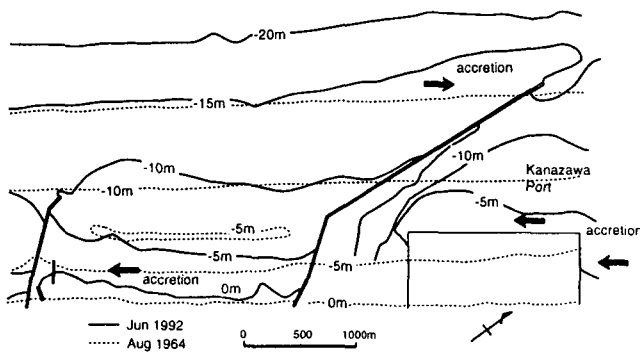


Fig. 6 Bottom topography change in the southern area of Kanazawa port